Isomers of Epidermal Growth Factor with Ser ⟹ Cys Mutation at the N-Terminal Sequence: Isomerization, Stability, Unfolding, Refolding, and Structure

Bao-Yuan Lu, Chuantao Jiang, and Jui-Yoa Chang*

Research Center for Protein Chemistry, Institute of Molecular Medicine, The University of Texas, Houston, Texas 77030

Received July 18, 2005; Revised Manuscript Received September 17, 2005

ABSTRACT: The structure of human epidermal growth factor (EGF, 53 amino acids) comprises three distinct loops (A, B, and C) connected correspondingly by the three native disulfide bonds, Cys^{6}−Cys^{20}, Cys^{14}−Cys^{31}, and Cys^{33}−Cys^{42}. The connection of Cys^{6} and Cys^{20} forming the N-terminal A loop is essential for the biological activity of EGF [Barnham et al. (1998) *Protein Sci. 7*, 1738−1749] and has also been shown to represent a major kinetic trap in the oxidative folding of EGF [Chang et al. (2001) *J. Biol. Chem. 276*, 4845−4852]. To further understand the chemical nature of this kinetic trap, we have prepared three EGF mutants each with a single Ser ⟹ Cys mutation at Ser residues (Ser^{2}, Ser^{4}, and Ser^{9}) flanking Cys^{6}. This allows competition between Cys^{6} and mutated Cys^{2}, Cys^{4}, and Cys^{9} to link with Cys^{20} and to form EGF isomers containing different sizes of the A loop. The results show that, in the cases of EGF-(S2C) and EGF(S4C), native Cys^{6}−Cys^{20} is favored over Cys^{2}−Cys^{20} and Cys^{4}−Cys^{20} by 4.5- and 9-fold, respectively, in the state of equilibrium. However, in the case of EGF(S9C), a non-native Cys^{9}−Cys^{20} is thermodynamically more stable than the native Cys^{6}−Cys^{20} by a free-energy difference ($\Delta G°$) of 1.12 kcal/mol. Implications of these data in the formation of kinetic trap of EGF folding are discussed. Stabilized isomers of EGF were further generated from denaturation of wild-type and mutant EGF via the method of disulfide scrambling. Properties of these diverse isomers of EGF, including their isomerization, stability, unfolding, refolding, and disulfide structures, are described in this paper.

Human epidermal growth factor (EGF)[1] stimulates the growth of epidermal and epithelial cells by binding to the EGF receptor (*1*, *2*). The EGF-like domain has been found in a large number of functional unrelated proteins. It occurs in more than 300 different sequences (*3*−*11*), ranging from urokinase, E-selectins, lipoprotein receptor, type-α transforming growth factor (TGF-α), heregulin, tissue plasminogen activator, and several factors involved in blood clotting.

EGF is a 6-kd (53 amino acids) polypeptide and is stabilized by three disulfide bonds with the pairing pattern of (1−3, 2−4, and 5−6) (Cys^{6}−Cys^{20}, Cys^{14}−Cys^{31}, and Cys^{33}−Cys^{42}) (*12*, *13*). Native EGF adopts a well-defined 3D structure and comprises three distinct loops (*12*, *14*). The N-terminal A loop (residues 6−19) contains some α-helical structure and is fastened by Cys^{6}−Cys^{20}. The B loop (residues 20−31) forms a two-stranded antiparallel β sheet. The C loop (residues 33−42) is constrained by a third disulfide bond Cys^{33}−Cys^{42}. The native conformation of EGF, like many small disulfide proteins, is determined essentially by its amino acid sequence alone (*15*). Fully reduced and denatured EGF is able to refold via disulfide oxidation to form the native conformation spontaneously and quantitatively (*16*−*18*). However, the folding mechanism of EGF displays unique properties that are not shared by many small disulfide proteins (*19*−*25*). Oxidative folding of the fully reduced EGF undergoes heterogeneous and transient 1-disulfide intermediates and accumulates rapidly as a single stable 2-disulfide kinetic trap (designated as EGF-II) (*16*), which represents up to more than 85% of the total protein along the folding pathway. EGF-II contains two free cysteines (Cys^{6} and Cys^{20}) and two native disulfide bonds of EGF, Cys^{14}−Cys^{31} and Cys^{33}−Cys^{42}. However, the formation of the third native disulfide (Cys^{6}−Cys^{20}) for EGF-II is exceedingly slow and does not occur directly. Kinetic analysis reveals that an important route for EGF-II to reach the native structure is to undergo substantial unfolding via the rearrangement pathway through 3-disulfide scrambled isomers (*16*). Thus, for EGF-II to escape the kinetic trap and convert to the native EGF, it will have to cross an energy barrier that would entail extensive unfolding of the already attained nativelike structure in EGF-II. In this case, native EGF is likely to be only marginally more stable than EGF-II. The difficulty of forming Cys^{6}−Cys^{20} is also consistent with its preferential and selective reduction in the process of reductive unfolding (*16*, *26*). In addition, the formation of Cys^{6}−Cys^{20} is required for EGF to form an active A loop (residues 6−19) that interacts with site 2 in domain III of EGF receptor (EGFR). Specifically, Leu^{15} and Tyr^{13} of the EGF A loop bind to Val^{350} and Phe^{357} of EGFR, respectively, via a hydrophobic interaction (*14*). Absence of this A loop has been shown in a synthetic analogue of murine EGF to significantly decrease the mitogenic activity and EGF receptor-binding affinity (*27*).

* To whom correspondence should be addressed: Institute of Molecular Medicine, 2121 W. Holcombe Blvd., Houston, TX 77030. E-mail: rowen.chang@uth.tmc.edu. Telephone: 713-500-2458. Fax: 713-500-2424.

[1] Abbreviations: EGF, epidermal growth factor; HPLC, high-performance liquid chromatography; GdmCl, guanidine hydrochloride; LCI, leech-derived carboxypeptidase inhibitor; DTT, dithiothreitol.

10.1021/bi051399c CCC: $30.25
Published on Web 10/22/2005

Table 1: Primers Used in QuickChange Site-Directed Mutagenesis Reactions

species	primers
S2C	5′-GAA CAA CAT ATG AAT TGT GAC TCT GAA TGT CCC-3′
	5′-GGG ACA TTC AGA GTC ACA ATT CAT ATG TTG TTC-3′
S4C	5′-CATATG AAT AGT GAC TGT GAA TGT CCC CTG TCC-3′
	5′-GGACAG GGG ACA TTC ACA GTC ACT ATT CAT ATG-3′
S9C	5′-TCT GAA TGT CCC CTG TGC CAC GAT GGG TAC TGC-3′
	5′-GCA GTA CCC ATC GTG GCA CAG GGG ACA TTC AGA-3′
A25C	5′-TGC ATG TAT ATT GAA TGC TTG GAC AAG TAT GCA-3′
	5′-TGC ATA CTT GTC CAA GCA TTC AAT ATA CAT GCA-3′

The presence of the major kinetic trap (EGF-II) of EGF folding and the unique conformational property of the N-terminal sequence of EGF surrounding Cys^6 suggest that further studies are necessary to understand the stability of EGF surrounding Cys^6-Cys^{20}. In this study, we attempt to alter the size of the A loop of EGF and to evaluate its effect on the conformational stability of EGF. To achieve this goal, we have selected three Ser residues at the vicinity of Cys^6 (Ser^2, Ser^4, and Ser^9) for Ser ⟹ Cys point mutations. The extra Cys^2, Cys^4, or Cys^9 shall then be allowed to compete with Cys^6 for disulfide linkage with Cys^{20}. This should in practice generate EGF isomers with enlarged and reduced sizes of A loop. An additional mutant with Ala^{25} ⟹ Cys replacement at the B loop was also produced as a control.

MATERIALS AND METHODS

Materials. Oligonucleotides were purchased from MWG-Biotech (NC). Lambda EGF116 Purified Phage DNA was purchased from ATCC (VA). All PCR reagents and restriction endonucleases were from Roche Applied Science (IL). QuickChange Site-Directed Mutagenesis Kit was obtained from Stratagene (CA). NAP-5 desalting column, Q-Sepharose Fast Flow, and Superdex G75 were from Amersham Biosciences (NJ). All other chemicals were of analysis or molecular biology grade. Plasmid pRBI-PDI-T7 was a gift from Dr. Rudi Glockshuber (Zurich, Switzerland).

Expression of Recombinant EGF Proteins. The gene coding for human EGF protein was amplified by the polymerase chain reaction from a construct of lambdaEGF116 phage DNA (*28*) using the following primers: N-terminal primer, 5′-CGA GAA CAA CAT ATG AAT AGT GAC TCT GAA TGT CCC CTG-3′; and C-terminal primer, 5′-GCA GCC GGA TCC TAC TAG CGC AGT TCC CAC CAC TTC AGG-3′. The amplified gene was cloned into the plasmid pRBI-PDI-T7 (*29*) via the *Nde*I and *Bam*HI restriction sites. The expressed EGF protein contains an additional amino acid residue of methionine at its amino terminus. The correct sequence of the amplified gene was verified by dideoxy sequencing.

Point mutations at S2C, S4C, S9C, and A25C were achieved using the QuickChange Site-Directed Mutagenesis reactions, respectively. All primers used for the mutagenesis reactions are listed in Table 1. The obtained plasmid DNAs were also verified by dideoxy sequencing. The obtained construct was then transformed into *Escherichia coli* BL21-(DE3), which were grown at 37 °C in LB medium containing carbenicillin (100 mg/L). At an optical density at 550 nm of 1.0−1.3, IPTG was added to a final concentration of 1 mM and then the cultures were grown for 16 h at 37 °C. Cells were harvested by centrifugation and resuspended in a lysis buffer (150 mM NaCl, 5 mM EDTA, 1 mM PMSF, and 50 mM Tris-HCl at pH 8.0). They were disrupted in a French Pressure Cell, and the lysate was centrifuged (4 °C, 39000*g*, 45 min).

The obtained inclusion bodies were washed twice with the same lysis buffer as described above and then solubilized in 8 M urea, 10 mM Tris-HCl at pH 8.0 containing 1 mM EDTA and 10 mM dithiothreitol (DTT). After centrifugation and filtration through a 0.2 μm syringe filter, the supernatant was applied to a Q-Sepharose Fast Flow column (20 mL) equilibrated with 8 M urea and 20 mM Tris-HCl at pH 8.0 and eluted with a linear NaCl gradient (400 mL, 0−600 mM). Fractions containing the EGF protein were combined, and the buffer was changed to 50 mM Tris-HCl (pH 8.0) using an Amicon ultrafiltration system. The sample was applied to a Superdex G-75 column equilibrated with 50 mM Tris-HCl (pH 8.0) and eluted with the same buffer. Fractions of the EGF protein were pooled again and concentrated by Amicon ultrafiltration. For structural (disulfide) analysis and an unfolding experiment, the obtained product was further purified by RP-high-performance liquid chromatography (HPLC) at a semipreparative scale on Agilent 1100 HPLC system (Column ZORBAX 3000 SB-C18 9.4 mm × 25 cm). Buffer A was 0.088% TFA in water, and buffer B was 0.084% TFA in 90% acetonitrile. The gradient was from 28% B to 44% B in 20 min at a flow rate of 2 mL/min. Purified proteins were freeze-dried and stored at −20 °C. The purified proteins were then verified by N-terminal Edman sequencing and mass spectrometry analysis. Typically, about 7.0 mg of EGF(S2C) and EGF(S4C), 3.0 mg of EGF(S9C), and 8.0 mg of EGF(A25C) were produced from 1 L of LB media after HPLC purification.

Chemical and Thermal Denaturation of Native N-EGF-(WT) and N-EGF(Mutants) via Disulfide Scrambling. N-EGF(WT) (0.5 mg/mL) was denatured at 22 °C in the Tris-HCl buffer (0.1 M, pH 8.4) containing 6 M guanidine hydrochloride (GdmCl) and different concentrations of Cys (80, 250, and 1000 μM). Denatured samples were quenched at a different time point by introduction of 2 volumes of 4% aqueous trifluoroacetic acid. N-EGF(mutants) (0.5 mg/mL) were denatured at 22 °C in the Tris-HCl buffer (0.1 M, pH 8.4) containing different concentration of GdmCl, without any supplementing thiol. Denaturation was carried out for 5 min and similarly quenched by acidification. Alternatively, N-EGF(mutants) (0.5 mg/mL) were also denatured at 80 °C for 5 min in the Tris buffer without supplementing thiol. All denatured samples were analyzed by RP-HPLC. The denaturation curve was determined by fractions (%) of the native EGF converted to the scrambled isomers. Quantitative analysis of the relative yield of scrambled and the

native isomer was based on the integration of HPLC peak areas.

Refolding of Denatured EGF Isomers via Disulfide Scrambling. Scrambled isomers of denatured EGF were purified from acid-trapped samples by RP-HPLC, freeze-dried, and allowed to carry on the folding by dissolving the sample (0.5 mg/mL) back into the Tris-HCl buffer (0.1 M, pH 8.4). Folding intermediates were trapped by mixing aliquots of the sample with 2 volumes of 4% aqueous trifluoroacetic acid at different time point and analyzed by HPLC.

Modification of EGF Proteins with Vinylpyridine. Isomers of EGF(mutants) intended for the biological assay were modified with vinylpyridine (10 μL) in 100 μL of Tris-HCl buffer (0.1 M, pH 8.4). Reactions were allowed at 23 °C for 45 min, acidified with 2 volumes of 4% aqueous trifluoroacetic acid, and purified by RP-HPLC or desalted through a NAP-5 column eluted with 0.1% trifluoroacetic acid. Fractions collected were freeze-dried and used for further analysis.

Analysis of Disulfide Structures of EGF Isomers. Protein samples (~10 μg) were isolated and treated with 1 μg of thermolysin in 30 μL of *N*-ethylmorpholine/acetate buffer (50 mM, pH 6.4). Digestion was carried out at 37 °C for 16 h. Thermolytic digests were quenched with 2 volumes of 4% aqueous trifluoroacetic acid, separated by HPLC, and analyzed by Edman sequencing and MALDI mass spectrometry. The digests were also analyzed by LC−MS (Agilent 1100 Series LC/MSD Trap). Data analysis were performed using the software provided by Bruker Daltonics.

Amino Acid Sequencing and Mass Spectrometry. The amino acid sequence of disulfide-containing peptides was analyzed by automatic Edman degradation using a Perkin−Elmer Procise sequencer (Model 494) equipped with an on-line PTH−amino acid analyzer. The molecular mass of peptides were determined by MALDI−TOF mass spectrometer (Perkin−Elmer Voyager-DE STR).

Nomenclature of Isomers of EGF Proteins. The nomenclature of isomers of EGF proteins is differentiated by symbols added at both the prefix and suffix. N-EGF and n-EGF stand for thermodynamically the first and second most stable native isomers at nondenaturing conditions. N-EGF(WT) and N-EGF(S2C) represent wild-type and $Ser^2 \Rightarrow Cys$ mutated N-EGF, etc. Scrambled species of EGF are designated by the following formula: X-EGF(point mutation) − (isomer assigned on HPLC), where X stands for scrambled. For instance, X-EGF(S9C)-b represents isomer "b" of scrambled EGF with a $Ser^9 \Rightarrow Cys$ point mutation.

RESULTS

Production and Verification of Oxidized EGF(Mutants). EGF proteins were expressed in the cytoplasm of *E. coli* BL21(DE3) and accumulated as inclusion bodies. After solubilization in 8 M urea (at pH 8.0) and purified by anion-exchange chromatography in the presence of urea, reduced EGF proteins were folded to form the nativelike disulfide bonds spontaneously after removing the denaturant. Folded proteins were purified subsequently by gel-filtration chromatography and were modified with vinylpyridine to determine the accessibility of the free amino acid residue cysteine.

Table 2: Molecular Weight of Recombinant EGF Mutants before and after Modification with Vinylpyridine

EGF(mutants)	before modification observed (expected)	after modification observed (expected)
N-EGF(S2C)	6363.3 (6363.4)	6468.8 (6468.5)
N-EGF(S4C)	6363.2 (6363.4)	6468.8 (6468.5)
N-EGF(S9C)	6363.6 (6363.4)	6468.5 (6468.5)
N-EGF(A25C)	6378.5 (6379.4)	6484.6 (6484.5)

Both unmodified and vinylpyridine-modified protein samples were subjected to MALDI−MS analysis. The data (Table 2) verify the correct molecular mass of all four EGF(mutants) and indicate a difference of 105.1 Da between unmodified and modified proteins in all cases. These results thus confirm the presence of a single free cysteine in each of the EGF mutants. The matured EGF domain contains 53 amino acids and 3 disulfide bonds (6 cysteines). In this paper, the recombinant EGF proteins were engineered from the EGF gene by PCR and bear a starting amino acid residue Met. Therefore, the expressed proteins all have 54 amino acids with a calculated molecular weight of 6369.26 Da (6363.26 Da in the oxidized form). However, to compare with the wide-type counterpart, the numbering of the amino acid sequence still starts with Asn (N1) and ends with Arg (R53) (see Figure 2).

Folded EGF(mutants) were further characterized by RP-HPLC (Figure 1). EGF(A25C) forms a single major isomer, designated as N-EGF(A25C). For the three Ser ⇒ Cys mutated EGF, however, each was shown to fold into one predominant isomer (designated as N-EGF) and a minor isomer (designated as n-EGF) that constitutes about 10−18% of the mutant protein. All n-EGF(mutants) exhibit a molecular mass identical to that of corresponding N-EGF-(mutants), both in unmodified and vinylpyridine-modified form, indicating that n-EGF(mutants) are isomers of N-EGF-(mutants) and also possess one free cysteine. For each Ser ⇒ Cys mutated EGF, these two isomers [n-EGF(mutants)/N-EGF(mutants)] are formed in the refolding mixture at the equilibrium, with an equilibrium constant (K_{eq}) of 0.22 for EGF(S2C), 0.11 for EGF(S4C), and 0.15 for EGF(S9C). These K_{eq} values correspond to a free-energy difference ($\Delta G°$) of 0.89, 1.30, and 1.12 kcal/mol, respectively.

Disulfide Structures of N-EGF(Mutants) and n-EGF-(Mutants). N-EGF(mutants) and n-EGF(mutants) of the four mutant proteins were isolated from RP-HPLC, derivatized with vinylpyridine, and directly subjected to 10 cycles of Edman sequencing. They were further fragmented by thermolysin digestion. Peptides were analyzed by LC−MS as well as Edman sequencing to identify those containing disulfide bonds and vinypiridine-modified cysteine. The data (available upon request) lead to the conclusion of the disulfide structures presented in Figure 2. N-EGF(S2C), N-EGF(S4C), and N-EGF(A25C) adopt a disulfide pattern identical to that of wild-type N-EGF and each contain a free cysteine at sequence positions 2, 4, and 25, as expected. The structure of N-EGF(S9C) is different. It is stabilized by a non-native disulfide bond (Cys^9-Cys^{20}) instead of native disulfide (Cys^6-Cys^{20}) and has a free cysteine at position 6.

n-EGF(S2C) and n-EGF(S4C) both have a free Cys at position 6. Each comprises two native disulfide bonds and a non-native disulfide bond, Cys^2-Cys^{20} and Cys^4-Cys^{20},

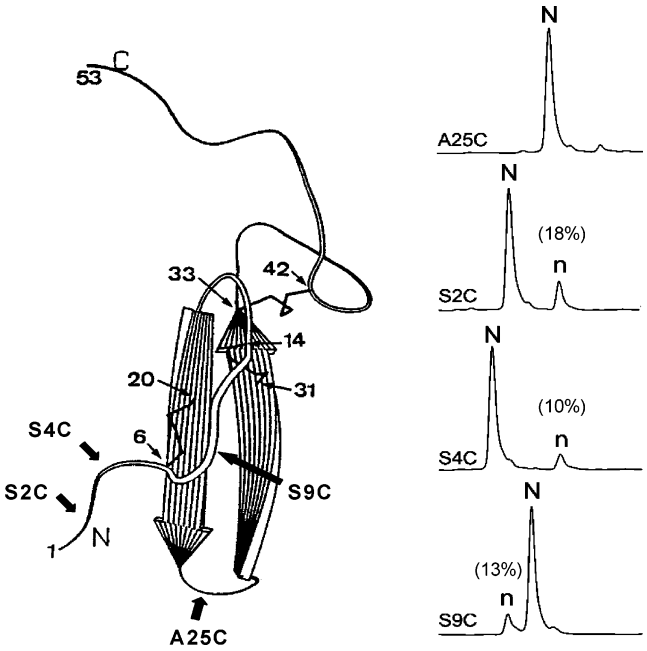

FIGURE 1: (Left) Schematic views of the native structure of human EGF (WT). N and C indicate the locations of N- and C-terminal regions of EGF. The three corresponding native disulfides, Cys^{6}-Cys^{20}, Cys^{14}-Cys^{31}, and Cys^{33}-Cys^{42} are numbered. The solid-bold arrows point to the positions of Ser/Ala ⇒ Cys mutation. Native EGF comprises three distinct loops. The N-terminal A loop (residues 6−19) is connected by Cys^{6}−Cys^{20}. The B loop (residues 20−31) forms a two-stranded antiparallel β sheet. The C loop (residues 33−42) is constrained by a third disulfide bond Cys^{33}−Cys^{42}. (Right) Analysis of purified EGF(mutants) by RP-HPLC. "N" and "n" stand for thermodynamically the first and second most stable native isomers. Analysis was performed on an Agilent 1100 series HPLC system using the following conditions. Solvent A was water containing 0.088% trifluoroacetic acid. Solvent B was acetonitrile/water (9:1, v/v) containing 0.084% trifluoroacetic acid. The gradient was 28−35% of solvent B linear in 15 min, 35−40% of solvent B linear in 15−45 min, and 40−80% of solvent B linear in 45−70 min. The column was Zorbax 300-SB C18, 4.6 × 250 mm, 5 μm. The flow rate was 0.2 mL/min. The column temperature was 22 °C.

respectively. In contrast, the disulfide pattern of **n**-EGF(S9C) is similar to that of N-EGF(WT) (Figure 2).

Denaturation and Unfolding of N-EGF(WT) and N-EGF-(Mutants) via Disulfide Scrambling. Denaturation and unfolding of N-EGF(WT) via disulfide scrambling requires the presence of supplementing thiol (Cys, GSH, or β-mercaptoethanol). Without supplementing thiol, N-EGF(WT) remains completely intact for up to 48 h in the buffer containing 8 M GdmCl (data not shown). Thermodynamic denaturation of N-EGF(WT) in the presence of a thiol catalyst at an increasing concentration of GdmCl have been investigated previously (*30*), and the data are used here to construct its denaturation curve (see Figure 6) and conformational stability for comparison with N-EGF(mutants) (Table 3). In this study, kinetics of denaturation of N-EGF-(WT) by 6 M GdmCl in the presence of different concentrations of thiol catalyst (80, 250, and 1000 μM Cys) were further investigated (Figure 3). At 80 μM Cys, denaturation of N-EGF(WT) is extremely slow and the reaction was brought to a halt after 4 h, presumably because of the depletion of Cys by air oxidation. At 250 and 1000 μM Cys, denaturation of N-EGF(WT) completed within 4 and 1 h, respectively. Denatured N-EGF(WT) consists of eight iden-

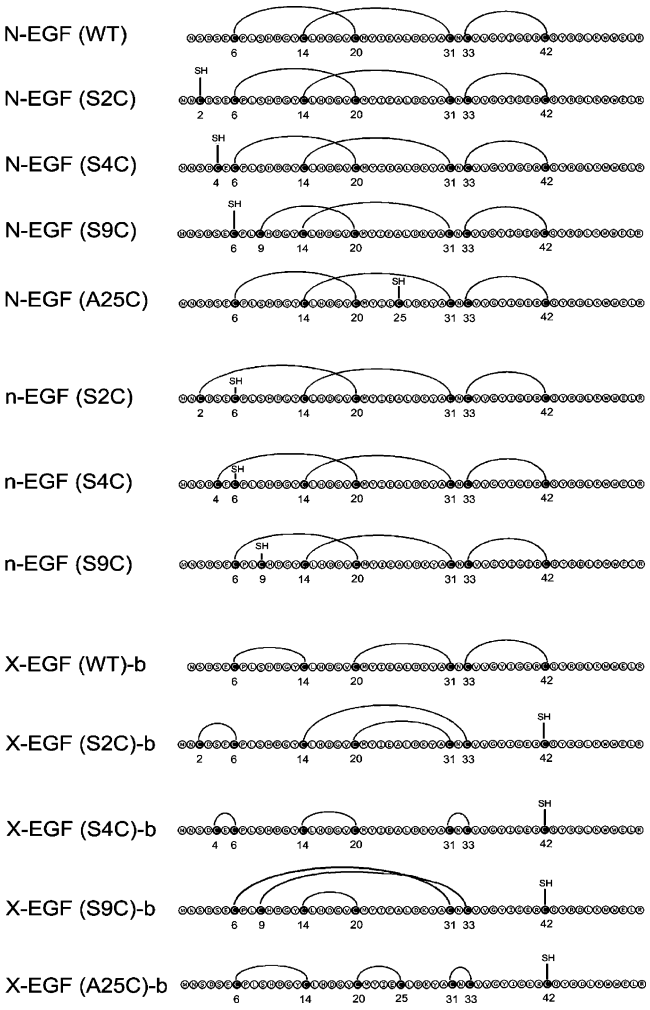

FIGURE 2: Disulfide structures of native and scrambled isomers of EGF(mutants) proteins. Their structures were derived from the LC−MS analysis of thermolysin-digested peptides. N-EGF(mutants) and n-EGF(mutants) indicate the most and second most predominant isomers in the absence of the denaturant (see Figure 1). X-EGF-(mutants)-b represents the major denatured isomer in the presence of 8 M GdmCl (see Figure 4). The position of free cysteine is indicated by SH.

Table 3: Differences in Stability between Wild-Type and Mutants EGF

protein	ΔG (H_2O)[a]	m[b]	$[GdmCl]_{1/2}$[c]
N-EGF(WT)	2.92	0.71	4.1
N-EGF(S2C)			
N-EGF(S4C)	1.41	0.52	2.7
N-EGF(S9C)			
N-EGF(A25C)	1.48	0.74	2.0

[a] In kcal/mol. [b] In kcal mol^{-1} M^{-1}. [c] Midpoint of the GdmCl unfolding curve in molars.

tifiable scrambled isomers. Their disulfide structures were characterized in our previous paper (*30*). Among them, the most predominant scrambled species, designated as X-EGF-(WT)-b (Figure 2) adopts the beads-form disulfide pattern.

When an extra cysteine, which serves as thiol catalyst, is introduced, N-EGF(mutants) may undergo rapid disulfide isomerization without any supplementing thiol. Inclusion of additional thiol is unnecessary and may actually cause an undesirable effect. It leads to the formation of a mixed disulfide adduct of all scrambled isomers, a phenomenon that

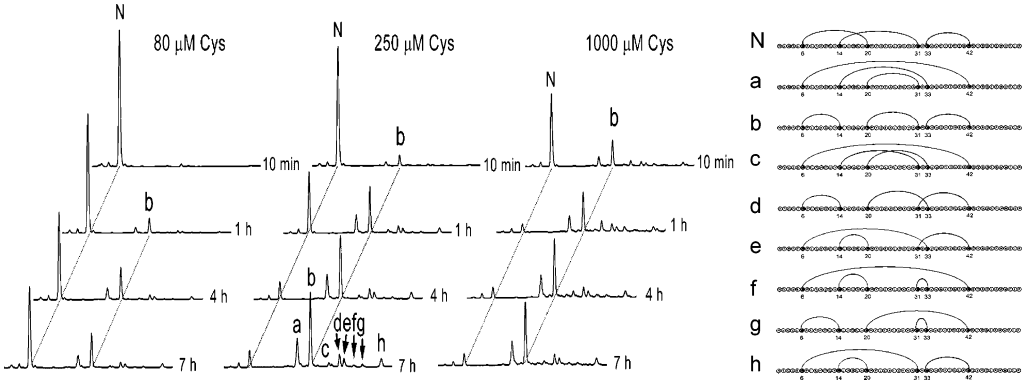

FIGURE 3: Denaturation of N-EGF(WT) by 6 M GdmCl in the presence of different concentrations of Cys. Denaturation was performed at 22 °C in the Tris-HCl buffer (0.1 M, pH 8.4) containing 80, 250, or 100 μM Cys. Denatured samples were quenched in a time course manner by acidification and analyzed by HPLC using conditions similar to those described in Figure 1, except for employing a different gradient system, which was 14−34% solvent B linear in 15 min and 34−56% solvent B linear from 15 to 50 min. "N" indicates N-EGF-(WT). Denatured N-EGF(WT) comprises eight fractions of scrambled isomers (marked by a, b, c, d, e, f, g, and h). Their disulfide structures have been characterized in a previous paper (*30*).

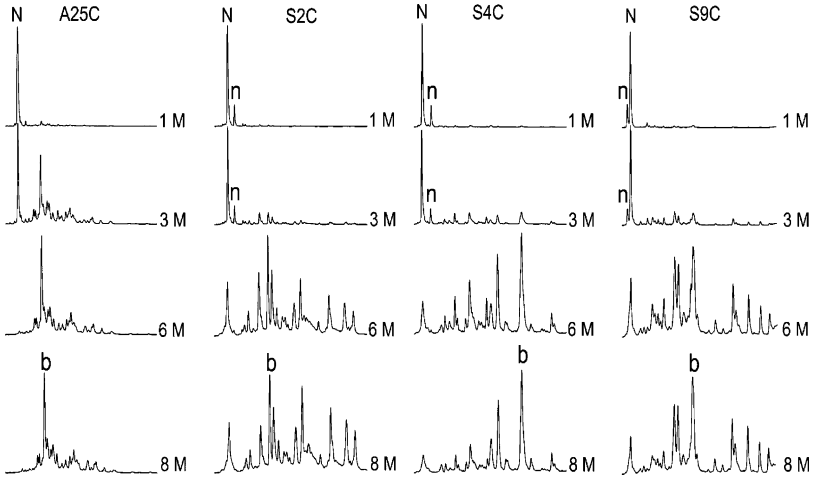

FIGURE 4: Denaturation of N-EGF(mutants) by an increasing concentration of GdmCl. Denaturation was carried out at 22 °C for 5 min in Tris-HCl buffer (0.1 M, pH 8.4) containing different concentrations of GdmCl. Reactions were quenched by mixing with 2 volumes of 4% trifluoreacetic acid and analyzed by HPLC. "b" indicates the most predominant isomer of denatured N-EGF(mutants).

has not been observed in the case of thiol-assisted denaturation of N-EGF(WT). The molecular mass of denatured scrambled isomers of EGF(mutants), as measured by LC−MS, increase by 75, 119, and 305, respectively, when β-mercaptoethanol, cysteine, or GSH was included in the denatured samples.

Therefore, experiments of denaturation of N-EGF(mutants) described here were performed without the addition of any thiol reagent. N-EGF(mutants) were incubated in the Tris-HCl buffer containing an increasing concentration of GdmCl. Kinetics of denaturation is relatively fast. At a given concentration of GdmCl, the conversion of the native to scrambled isomers reaches equilibrium within about 5 min. Under these conditions, denatured isomers of EGF(mutants) all comprise only one free cysteine, as determined by LC−MS of vinylpyridine-trapped reaction mixtures (data not shown). Prolonged sample incubation resulted in a gradual decrease of the recovery of total proteins, possibly because of dimerization and precipitation of the protein. Figure 4 presents the HPLC profiles of denatured isomers of four N-EGF(mutants) obtained at different GdmCl concentrations. The results demonstrate that denaturation of all N-EGF-(mutants) occurs rapidly at around 3 M GdmCl. However, the heterogeneity of denatured isomers varies. Denatured EGF(A25C) consists of one predominant isomer designated as X-EGF(A25C)-b. In contrast, denatured EGF(S2C), EGF-(S4C), and EGF(S9C) each comprises about 25 fractions of well-populated isomers. Among them, the major species were also marked as X-EGF(S2C)-b, X-EGF(S4C)-b, and X-EGF-(S9C)-b, respectively. Heat-denatured EGF mutants are similarly heterogeneous (Figure 5). The higher heterogeneity of denatured EGF(mutants) as compared to that of EGF-(WT) is predictable, because the presence of an extra cysteine increases the number of potential scrambled isomers from 14 to 104.

Denaturation Curves of N-EGF(WT) and N-EGF(Mutants). The method of disulfide scrambling permits quantitative analysis of the denaturation curve and unfolding curve independently (*16*). In this study, denaturation curves of EGF(mutants) are determined by the fraction (%) of the native isomer ("N" species) converted to the scrambled isomers (collectively designated as "X") under a rising temperature (40−80 °C) or increasing concentrations of GdmCl (1−8 M). Quantitative analysis of the relative yield of scrambled and the native isomers was based on the integration of HPLC peak areas. The denaturation curves of

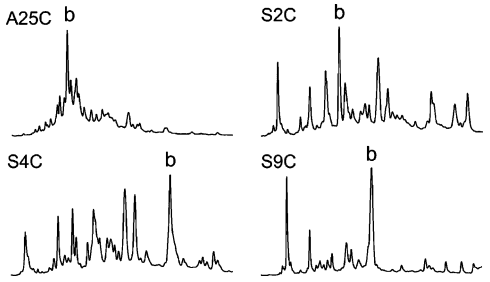

FIGURE 5: Denaturation of N-EGF(mutants) at elevated temperature. Denaturation was performed at 80 °C for 5 min in Tris-HCl buffer (0.1 M, pH 8.4). Reactions were quenched by mixing with 2 volumes of 4% aqueous trifluoreacetic acid and analyzed by HPLC. "b" indicates the most predominant isomer of denatured N-EGF-(mutants).

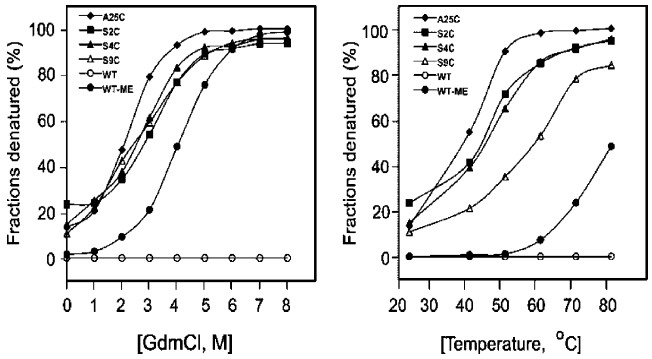

FIGURE 6: Denaturation curves of EGF proteins at a rising temperature (right) and in the presence of increasing concentrations of GdmCl (left). Fractions denatured indicate the fraction (%) of native protein converted to scrambled species, calculated from HPLC analysis as shown on Figure 4. All denaturation experiments of N-EGF(mutants) were performed without supplementing thiol. N-EGF(A25C) (◆), N-EGF(S2C) (■), N-EGF(S4C) (▲), and N-EGF(S29C) (△). Denaturation of wild-type N-EGF in the presence (●, WT-ME) and absence (○, WT) of β-mercaptoethanol (0.2 mM) are included as controls. In these analysis, the "n" isomers of EGF(mutants) are counted as denatured species.

N-EGF(WT) analyzed in the presence of β-mercaptoethanol (0.2 mM) are included as a control for comparison. Denaturation of EGF(mutants) undergoes a two-stage mechanism. The three Ser ⇒ Cys EGF(mutants) exhibit a comparable stability against GdmCl (Figure 6, left), all with a 50% denaturation that occurs at around 2.7 M GdmCl. Midpoint denaturation of N-EGF(A25C) occurs at 2 M GdmCl. Their decreased stability contrasts to that of N-EGF(WT), which requires 4 M GdmCl to achieve 50% denaturation.

The data of thermal denaturation further demonstrate variation of conformational stability between N-EGF(WT) and N-EGF(mutants) (Figure 6, right). All mutants are considerably less stable than wild-type EGF. However, in these experiments, N-EGF(S9C), which contains a non-native disulfide bond, displays a noticeably higher thermal stability than both N-EGF(S2C) and N-EGF(S4C).

Calculation of Conformational Stability of N-EGF(WT) and N-EGF(Mutants). The conformational stability of N-EGF(mutants) in the absence of the denaturant (ΔG^{H_2O}) is determined from the GdmCl denaturation curves (Figure 5). Despite limited concentration points of GdmCl that were selected for the denaturation studied, the data provide F_u (fractions unfolded or fractions denatured) at each point of GdmCl and allow an estimation of the difference in free energy (ΔG_{app}) between the folded and unfolded conformations, which was calculated using

$$\Delta G_{app} = -RT \ln[(F_u)/(1 - F_u)]$$

Least-squares analysis was used to fit the data to the equation

$$\Delta G_{app} = \Delta G^{H_2O} - m[\text{GdmCl}]$$

where ΔG^{H_2O} is the value of ΔG_{app} in the absence of GdmCl and m is the measure of the dependence of ΔG_{app} on the GdmCl concentration. The correlation of the midpoint of the GdmCl denaturation curve and ΔG^{H_2O} was calculated by the equation $[\text{GdmCl}]_{1/2} = [(\Delta G^{H_2O})/m]$, because $\Delta G_{app} = 0$ at $[\text{GdmCl}]_{1/2}$. Results are summarized in Table 3.

Disulfide Structures of the Major Isomers of Denatured EGF(Mutants). Four major denatured isomers of EGF-(mutants), X-EGF(S2C)-b, X-EGF(S4C)-b, X-EGF(S9C)-b, and X-EGF(A25C)-b, were isolated from HPLC, modified with vinylpyridine, and subject to thermolysin digestion. Peptide mixtures were analyzed by LC−MS. Data obtained lead to the conclusion of their disulfide structures presented in Figure 2. All four scrambled species leave a free cysteine at position 42, indicating that, even at the denatured state, the N-terminal sequence of EGF(mutants) is more likely to exist in a more compact structure than that of the C-terminal region. X-EGF(S4C)-b and X-EGF(A25C)-b were shown to assume the "beads-form" disulfide structure, similar to that of X-EGF(WT)-b.

Scrambled Isomers of EGF(Mutants) Refold Spontaneously To Form the Native Disulfide-Bond Structure. Denatured isomers of EGF(mutants), because of the presence of a free cysteine, may refold spontaneously in the alkaline buffer without any supplementing thiol. Four scrambled isomers of EGF(mutants), X-EGF(S2C)-b, X-EGF(S4C)-b, X-EGF-(S9C)-b, and X-EGF(A25C)-b, were isolated from HPLC under acidic conditions, freeze-dried, and reconstituted in the Tris-HCl buffer (pH 8.4) to initiate the folding. Folding intermediates were quenched by acidification and analyzed by HPLC (Figure 7, middle and left panels). The results show that folding of the four isomers proceeds through heterogeneous intermediates to attain the native structure. Similar to the process of unfolding (denaturation), the kinetics of refolding of X-EGF(mutants) are relatively fast. Folding of all four isomers completes essentially within 10−20 min. For example, refolding of X-EGF(S2C)-b exhibits a first-order kinetics of 2.8×10^{-1} min^{-1}. The rate of recovery of N-EGF(S2C) and N-EGF(S4C) is about 2-fold faster than that of N-EGF(S9C) and N-EGF(A25C). The folded proteins consist of both "N" and "n" isomers with ratios indistinguishable from that shown in Figure 1, further indicating that these two isomers exist in a state of equilibrium in the absence of the denaturant.

For comparison, the refolding kinetic of X-EGF(WT)-b was analyzed in the presence of different concentrations of Cys (Figure 7, right panel). The results demonstrate that effective refolding of X-EGF(WT)-b occurs only in the presence of 1 mM Cys, a concentration about 12-fold of the protein (0.5 mg/mL). Under these conditions, refolding of X-EGF(WT)-b exhibits a first-order kinetics of 1.67×10^{-2} min^{-1}.

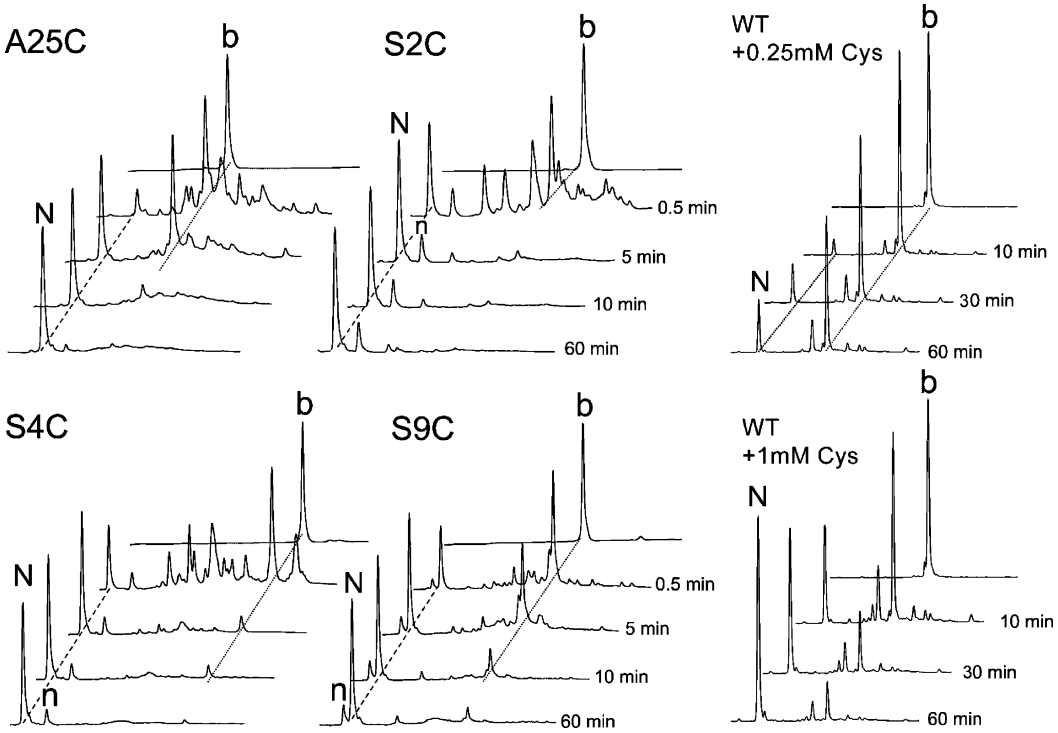

FIGURE 7: Refolding of scrambled EGF isomers. (Left and middle panels) X-EGF(S2C)-b, X-EGF(S4C)-b, X-EGF(S9C)-b, and X-EGF-(A25C)-b were allowed to refold at 22 °C in Tris-HCl buffer (0.1 M, pH 8.4). Supplementing thiol is not necessary in these reactions. (Right panel) Refolding of X-EGF(WT)-b was performed at 22 °C in Tris-HCl buffer, catalyzed by 0.25 mM and 1 mM Cys. All folding intermediates were trapped by sample acidification and analyzed by HPLC using the same conditions described in the caption of Figures 1 and 3. "N" indicates the refolded native proteins.

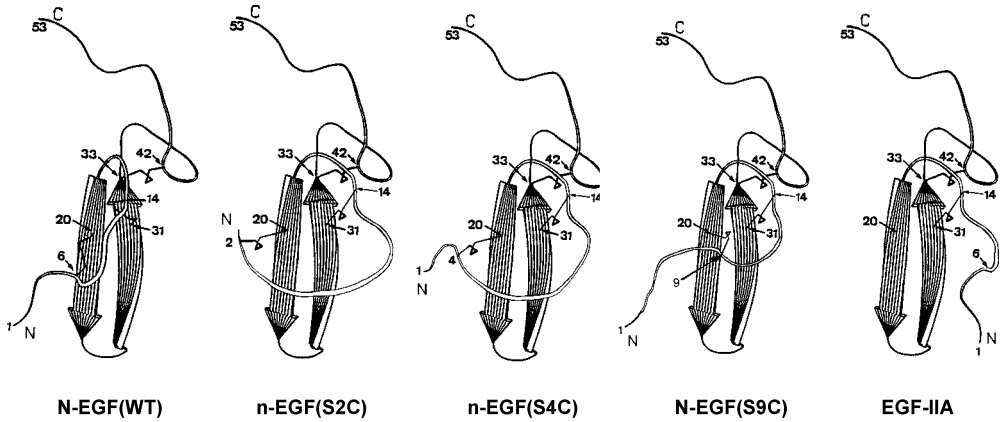

FIGURE 8: Schematic views of the putative structures of EGF-II and isomers of EGF with increased and decreased sizes of the N-terminal A loop. N and C indicate the locations of N- and C-terminal regions of EGF. The putative structure of EGF-II is based on the NMR structure of a synthetic analogue of murine EGF lacking Cys^6-Cys^{20}, [Abu6,20]mEGF4−48 (Abu denotes amino-butyric acid) (*27*). The structures of n-EGF(S2C), n-EGF(S4C), and N-EGF(S29C) are hypothetical models.

DISCUSSION

Molecular Mechanisms Accounting for the Major Kinetic Trap of EGF Folding. The N-terminal A loop of the human EGF structure (Figure 1) is connected by Cys^6-Cys^{20}. Formation of this loop, which is essential for the biological activity of EGF (*27*), represents a major and exclusive kinetic trap in the pathway of oxidative folding of EGF (*16*, *17*). We have investigated here the effect of three Ser ⟹ Cys point mutations at Ser residues flanking Cys^6 on the structure and function of EGF. These studies have allowed preparation of three EGF isomers with either increased or decreased sizes of the N-terminal A loop (Figure 8). The results also reveal that an isomer [N-EGF(S9C)] with a smaller A loop connected by Cys^9-Cys^{20} is actually thermodynamically more stable than the one [n-EGF(S9C)] linked by the native Cys^6-Cys^{20} in the mutant EGF(S9C), with a free-energy difference ($\Delta G°$) of 1.12 kcal/mol. This unexpected finding should have implications on the accumulation of EGF-II as an exclusive kinetic trap of EGF folding (*16*).

EGF-II contains two native disulfide bonds of EGF, $Cys^{14}-Cys^{31}$ and $Cys^{33}-Cys^{42}$, and two free cysteines (Cys^6 and Cys^{20}). The molecular basis accounting for the specific property of EGF-II may be found in the NMR structure of a synthetic analogue of murine EGF lacking Cys^6-Cys^{20}, [Abu6,20]mEGF4−48 (Abu denotes amino-butyric acid) (*27*). The overall structure of [Abu6,20]mEGF4−48 is similar

to that of mEGF, indicating that the absence of Cys^6-Cys^{20} does not affect the global fold of EGF. However, the direction of the N-terminal segment of [Abu6,20]mEGF4−48, between residues four and nine, is located on the opposite face of the main β sheet from their position in the native mEGF (*27*). It is plausible that EGF-II may adopt a similar fold. A putative structure of EGF-II based on [Abu6,20]-mEGF4−48 is presented in Figure 8. This structure can be used to explain the stability of EGF-II as a kinetic trap and its inability to undergo direct Cys^6-Cys^{20} formation. The structure reveals that, in the absence of a connection of Cys^6 and Cys^{20}, the N-terminal sequence of EGF-II (residues 1−13) would prefer the conformation shown in Figure 8. For EGF-II to escape the kinetic trap and convert to the native EGF, it has to flip the N-terminal peptide form one side of the β sheet to the other. This will require EGF-II to cross an energy barrier that would entail extensive unfolding of the already attained nativelike structure in EGF-II. The major pathway, if not the only pathway, for EGF-II to reach the native structure is through 3-disulfide scrambled species (*16*). As such, the formation of a smaller disulfide loop linked by Cys^9-Cys^{20} should allow a greater entropy and thus enable N-EGF(S9C), a thermodynamically more stable isomer than n-EFGF(S9C) (Figure 1 and Figure 2).

EGF-II is not alone in its uniqueness. Two major kinetic traps identified along the folding pathway of leech-derived carboxypeptidase inhibitor (LCI) exhibit similar properties (*31*−*33*). LCI is a 4-disulfide protein. LCI-IIIA and LCI-IIIB are two 3-disulfide folding intermediates that accumulate along the pathway of oxidative folding of LCI. Both contain exclusively native disulfide bonds. Stop/go folding experiments have demonstrated that, for LCI-IIIA and LCI-IIIB to form the fourth native disulfide bonds, they will also have to unravel an existing nativelike structure and undergo 4-disulfide scrambled LCI as major intermediates to attain the native LCI (*32*).

Conformational Stability of N-EGF(WT) and N-EGF-(Mutants). Conformational stability of EGF was analyzed in this paper using the method of "*disulfide scrambling*" (*34*, *35*). N-EGF(WT) exhibits a midpoint denaturation at 4.1 M GdmCl, and its conformational stability (ΔG^{H_2O}) is estimated to be 2.92 kcal/mol. These data are in contrast to those obtained using the method of "*disulfide intact*" denaturation, which shows 50% denaturation of EGF at 6.9 M GdmCl and a rough estimate of unfolding free energy of 16 kcal/mol (*36*). This disparity is reminiscent of the conformational stability of phospholipase A_2 determined by these two different methods (*37*), in which 50% denaturation of phospholipase A_2 requires 2.5 and 6.4 M GdmCl, respectively. A higher conformational stability exhibited by the protein when denatured only by GdmCl in the absence of supplementing thiol was mainly due to the fact that the rigid disulfide network was not affected. Intact disulfides increase the conformational stability mainly by constraining the unfolded conformations of the protein and thereby decreasing their conformational entropy. When the denaturation was conducted in the presence of catalytic amounts of thiol, the native disulfide framework was "*teased*" to break and reform according to the conformational changes induced by the denaturant. Once the rigid "*native-framework*" of disulfides was rendered flexible, the conformational stability become mainly supported by the noncovalent interactions, which maintain the secondary and tertiary structure and supplemented the stability rendered by the disulfides.

Conformational stability of the four EGF(mutants) has also been analyzed by the method of "*disulfide scrambling*". However, instead of using a supplementing thiol as required for denaturing N-EGF(WT), the process of disulfide isomerization of N-EGF(mutants) is catalyzed by the extra mutated cysteine. Therefore, a comparison between EGF(WT) and EGF(mutants) is tricky at best. Nonetheless, the results reveal that all mutants are considerably less stable than the wild-type EGF. Within the experimental errors allowed (±5%), the results show that the midpoint denaturation (2.7 M GdmCl) and estimated ΔG^{H_2O} (1.41 kcal/mol) are roughly indistinguishable for the three Ser ⇒ Cys mutants. N-EGF-(A25C) needs only 2 M GdmCl to achieve 50% denaturation. However, its ΔG^{H_2O} (1.48 kcal/mol) is very close to that of Ser ⇒ Cys mutants, because the *m* value is greater (Table 3). It is noteworthy to mention that the "*m*" value associated with a folding/unfolding reaction is generally proportional to the change in solvent-accessible surface area between the folded and unfolded species. The fact that all three N-EGF-(mutants) exhibit an indistinguishable "*m*" value (with allowable variation of ±5%) (Table 3) suggests that their solvent-accessible surface have not been significantly affected because of either a Ser ⇒ Cys replacement (S2C and S4C mutants) or a size decrease of the A loop (S9C mutant).

Reversible Unfolding and Refolding of EGF(WT) and EGF(Mutants) Catalyzed by Supplementing Cys and Built-in Cys. A unique property of Ser ⇒ Cys EGF(mutants) is their rapid disulfide scrambling in the absence of any supplementing thiol. Unfolding and refolding of disulfide proteins via disulfide scrambling typically require the presence of free thiol as a catalyst (*34*, *35*). The thiol catalyst can be β-mercaptoethanol, GSH, or Cys, etc. It can be either supplementing free Cys or built-in protein Cys, such as mutated extra Cys of EGF(mutants) demonstrated in this paper. However, as the data demonstrated here, the potency of supplementing Cys and build-in Cys in promoting the disulfide scrambling differs significantly. The phenomenon has been observed both in the course of unfolding and refolding of all four EGF(mutants). This is best illustrated with the results shown in Figure 7. Refolding of purified X-EGF(S2C)-b, which is catalyzed by ~80 μM build-in Cys (derived from 0.5 mg/mL of EGF), exhibits a first-order kinetics of 2.8×10^{-1} min^{-1} and completes practically within 10 min. In contrast, refolding of X-EGF(WT)-b catalyzed by 1000 μM supplementing Cys displays a first-order kinetics of 1.67×10^{-2} min^{-1}. When the difference of both folding kinetics and the concentration of free thiol are taken into consideration, the disparity of potency between build-in Cys and supplementing Cys is an astounding 200-fold. Similar disparity is also observed in the process of unfolding between N-EGF(WT) and N-EGF(mutants). For example, GdmCl (6 M) unfolding of all four N-EGF(mutants) catalyzed by ~80 μM build-in Cys (0.5 mg/mL of EGF) accomplishes within 5 min (Figure 4). Similar GdmCl unfolding of N-EGF(WT) in the presence of 1000 μM supplementing Cys completes only after about 45 min of reaction (Figure 3). Again, when the difference of unfolding kinetics and the concentration of free Cys are factored in, the difference of effectiveness between build-in Cys and supplementing Cys is greater than 120-fold.

This discrepancy may be due in part to the favored redox potential of mutated Cys of EGF, but most likely it is a consequence of the localized accessibility (concentration) of build-in Cys to disulfide bonds that undergo disulfide scrambling, a property that further indicates the conformational dynamism and flexibility of scrambled proteins. An additional explanation is the different reaction order involved in these two cases. When the disulfide bond reshuffling is promoted by an externally supplemented Cys, a bimolecular reaction is required. When the reshuffling is catalyzed by the build-in Cys, the reaction is essentially intramolecular. Similar phenomenon of build-in Cys-promoted disulfide shuffling has been observed in the production of the hirudin dimer (*38*) and the folding of pro BPTI (*39*, *40*).

ACKNOWLEDGMENT

The authors acknowledge the support from the Protein Institute, Inc. and the Robert Welch foundation.

REFERENCES

1. Carpenter, G. (1987) Receptors for epidermal growth factor and other polypeptide mitogens, *Annu. Rev. Biochem. 56*, 881−914.
2. Schlessinger, J., and Ullrich, A. (1992) Growth factor signaling by receptor tyrosine kinases, *Neuron 9*, 383−391.
3. Doolittle, R. F., Feng, D. F., and Johnson, M. S. (1984) Computer-based characterization of epidermal growth factor precursor, *Nature 307*, 558−560.
4. Campbell, I. D., and Bork, P. (1993) Epidermal growth factor-like modules, *Curr. Opin. Struct. Biol. 3*, 385−392.
5. Hojrup, P., and Magnusson, S. (1987) Disulphide bridges of bovine factor X, *Biochem. J. 245*, 887−892.
6. Meininger, D. P., Hunter, M. J., and Komives, E. A. (1995) Synthesis, activity, and preliminary structure of the fourth EGF-like domain of thrombomodulin, *Protein Sci. 4*, 1683−1695.
7. Smith, B. O., Dowing, A. K., Driscoll, P. C., Dudgeon, T. J., and Campbell, I. D. (1995) The solution structure and backbone dynamics of the fibronectin type I and epidermal growth factor-like pair of modules of tissue-type plasminogen activator, *Structure 3*, 823−833.
8. Selande-Sunnerhagen, M., Ullner, M., Persson, E., Teleman, O., Stenflo, J., and Drakenberg, T. (1992) How an epidermal growth factor (EGF)-like domain binds calcium. High-resolution NMR structure of the calcium form of the NH2-terminal EGF-like domain in coagulation factor X, *J. Biol. Chem. 267*, 19642−19649.
9. Baron, M., Norman, D. G., Harvey, T. S., Handford, P. A., Mayhew, M., Tse, A. G. D., Brownlee, G. G., and Campbell, I. D. (1992) The three-dimensional structure of the first EGF-like module of human factor IX: Comparison with EGF and TGF-α, *Protein Sci. 1*, 81−90.
10. Moy, F. J., Li, Y.-C., Rauenbuehler, P., Winkler, M. E., Scheraga, H. A., and Montelione, G. T. (1993) Solution structure of human type-α transforming growth factor determined by heteronuclear NMR spectroscopy and refined by energy minimization with restraints, *Biochemistry 32*, 7334−7353.
11. Graves, B. J., Crowther, R. L., Chandran, C., Rumberger, J. M., Li, S., Huang, K.-S., Presky, D. H., Familletti, P. C., Wolitsky, B. A., and Burns, D. K. (1994) Insight into E-selectin/ligand interaction from the crystal structure and mutagenesis of the lec/EGF domains, *Nature 367*, 532−538.
12. Montelione, G. T., Wuthrich, K., Burgess, A. W., Nice, E. C., Wagner, G., Gibson, K. D., and Scheraga, H. A. (1992) Solution structure of murine epidermal growth factor determined by NMR spectroscopy and refined by energy minimization with restraints, *Biochemistry 31*, 236−249.
13. Hommel, U., Harvey, T. S., Driscoll, P. C., and Campbell, I. D. (1992) Human epidermal growth factor. High-resolution solution structure and comparison with human transforming growth factor α, *J. Mol. Biol. 227*, 271−282.
14. Ogiso, H., Ishitani, R., Nureki, O., Fukai, S., Yamanaka, M., Kim, J. H., Saito, K., Sakamoto, A., Inoue, M., Shirouzu, M., and Yokoyama, S. (2002) Crystal structure of the complex of human epidermal growth factor and receptor extracellular domains, *Cell 110*, 775−787.
15. Anfinsen, C. B. (1973) Principles that govern the folding of protein chains, *Science 181*, 223−230.
16. Chang, J.-Y., Li, L., and Lai, P.-H. (2001) A major kinetic trap for the oxidative folding of human epidermal growth factor, *J. Biol. Chem. 276*, 4845−4852.
17. Chang, J.-Y., Schindler, P., Ramseier, U., and Lai, P.-H. (1995) The disulfide folding pathway of human epidermal growth factor, *J. Biol. Chem. 270*, 9207−9216.
18. Wu, J., Yang, Y., and Watson, J. T. (1998) Trapping of intermediates during the refolding of recombinant human epidermal growth facyor (hEGF) by cyanylation and subsequent structural elucidation by mass spectrometry, *Protein Sci. 7*, 1017−1028.
19. Creighton, T. E. (1992) The disulfide folding pathway of BPTI, *Science 256*, 111−114.
20. Cemazar, M., Zahariev, S., Lopez, J. J., Carugo, O., Jones, J. A., Hore, P. J., and Pongor, S. (2003) Oxidative folding intermediates with nonnative disulfide bridges between adjacent cysteine residues, *Proc. Natl. Acad. Sci. U.S.A. 100*, 5754−5759.
21. Weissman, J. S., and Kim, P. S. (1991) Re-examination of the folding of BPTI: Predominance of native intermediates, *Science 253*, 1386−1393.
22. Rothwarf, D. M., Li, Y. J., and Scheraga, H. A. (1998) Regeneration of bovine pancreatic ribonuclease A: Detailed kinetic analysis of two independent folding pathways, *Biochemistry 37*, 3767−3776.
23. Chatrenet, B., and Chang, J.-Y. (1993) The disulfide folding pathway of hirudin elucidated by stop/go folding experiments, *J. Biol. Chem. 268*, 20988−20996.
24. Chang, J.-Y. (1996) The disulfide folding pathway of tick anticoagulant peptide, a kunitz-type inhibitor structurally homologous to BPTI, *Biochemistry 35*, 11702−11709.
25. Chang, J.-Y., Cannals, F., Schindler, P., Querol, E., and Aviles, F. X. (1994) The disulfide folding pathway of potato carboxypeptidase inhibitor, *J. Biol. Chem. 269*, 22087−22094.
26. Chang, J.-Y., Li, L., and Bulychev, A. (2000) The underlying mechanism for the diversity of disulfide folding pathways, *J. Biol. Chem. 275*, 8287−8289.
27. Barnham, K. J., Torres, A. M., Alewood, D., Alewood, P. F., Domagala, T., Nice, E. C., and Norton, R. S. (1998) Role of the 6−20 disulfide bridge in the structure and activity of epidermal growth factor, *Protein Sci. 7*, 1738−1749.
28. Bell, G. I., Fong, N. M., Stempien, M. M., Wormsted, M. A., Caput, D., Ku, L., Urdea, M. S., Rall, L. B., and Sanchez-Pescador, R. (1986) Human epidermal growth factor precursor: cDNA sequence, expression *in vitro*, and gene organization, *Nucleic Acid Res. 14*, 8427−8446.
29. Hornemann, S., Korth, C., Oesch, B., Riek, R., Wider G., Wurthrich, K., and Glockshuber, R. (1997) Recombinant full-length murine prion protein, mPrP(23−231): Purification and spectroscopic characterization, *FEBS Lett. 413*, 277−281.
30. Chang, J.-Y., and Li, L. (2002) The disulfide structure of denatured epidermal growth factor: Preparation of scrambled disulfide isomers, *J. Protein Chem. 21*, 203−213.
31. Salamanca, S., Li, L., Vendrell, J., Aviles, F. X., and Chang, J.-Y. (2003) Major kinetic traps for the oxidative folding of leech carboxypeptidase inhibitor, *Biochemistry 42*, 6754−6761.
32. Arolas, J. L., Bronsoms, S., Lorenzo, J., Aviles, F. X., Chang, J.-Y., and Ventura, S. (2004) Role of kinetic intermediates in the folding of carboxypeptidase inhibitor, *J. Biol. Chem. 279*, 37261−37270.
33. Arolas, J. L., Popowicz, G. M., Bronsoms, S., Aviles, F. X., Huber, R., Holak, T. A., and Ventura, S. (2005) Study of a major intermediate in the oxidative folding of leech carboxypeptidase inhibitor: Contribution of the fourth disulfide bond, *J. Mol. Biol. 352*, 961−975.
34. Chang, J.-Y. (1999) Denatured states of Tick anticoagulant peptide, *J. Biol. Chem. 274*, 123−128.
35. Chang, J.-Y., and Li, L. (2001) The structure of denatured α-lactalbumin elucidated by the technique of disulfide scrambling: Fractionation of conformational isomers of α-lactalbumin, *J. Biol. Chem. 276*, 9705−9712.
36. Holladay, L. A., Savage, C. R., Jr., Cohen, S., and Puett, D. (1976) Conformation and unfolding thermodynamics of epidermal growth factor and derivatives, *Biochemistry 15*, 2624−2633.
37. Singh, R. R., and Chang, J.-Y. (2004) Investigating conformational stability of bovine pancreatic phospholipase A_2. A novel concept

in evaluating the contribution of "native-framework" of disulfides to the global conformational stability of proteins, *Biochem. J. 377*, 685−692.
38. Chang, J.-Y., Grossenbacher, H., Meyhack, B., and Maerki, W. (1993) Production of disulfide-linked hirudin dimer by *in vitro* folding, *FEBS Lett. 336*, 53−56.
39. Weissman, J. S., and Kim, P. S. (1992) The pro region of BPTI facilitates folding, *Cell 71*, 841−851.
40. Bryan, P. N. (2002) Prodomains and protein folding catalysis, *Chem. Rev. 102*, 4805−4816.

BI051399C